

DMD#35824

COMPARATIVE USE OF ISOLATED HEPATOCYTES AND HEPATIC  
MICROSOMES FOR P450 INHIBITION STUDIES: TRANSPORTER-ENZYME  
INTERPLAY

Hayley S. Brown<sup>1</sup>, Alison J. Wilby<sup>2</sup>, Jane Alder<sup>3</sup> and J. Brian Houston

Centre for Applied Pharmacokinetic Research, School of Pharmacy and  
Pharmaceutical Sciences, University of Manchester, Manchester, United Kingdom

DMD#35824

**Running title:**

Transporter-enzyme interplay and inhibition assessment in vitro

**Corresponding Author:**

J Brian Houston  
Centre for Applied Pharmacokinetic Research  
School of Pharmacy and Pharmaceutical Sciences  
University of Manchester  
Manchester  
M13 9PT  
UK  
Tel: +44 (0) 161 275 8348  
Fax: +44 (0) 161 275 8349  
Email: [brian.houston@manchester.ac.uk](mailto:brian.houston@manchester.ac.uk)

Number of text pages:

Number of tables: 5

Number of figures: 4

Number of references: 40

Words in abstract: 249

Words in introduction: 734

Words in discussion: 1202

Abbreviations used are:

$CL_{int}$ , intrinsic clearance;  $f_u$ , fraction of unbound drug; CLAR, clarithromycin; DDI, drug-drug interaction; ENX, enoxacin;  $K_p$ , tissue-to-medium total drug concentration ratio;  $K_{p_u}$ , true hepatocyte-to-medium unbound drug concentration ratio reflecting purely distribution processes;  $K_{p_{u,app}}$ , apparent hepatocyte-to-medium unbound drug concentration ratio reflecting both elimination and distribution processes; NFV, nelfinavir; OATP, organic anion transporter polypeptide; SQV, saquinavir.

DMD#35824

## Abstract

Accurate assignment of the concentration of victim drug/inhibitor available at the enzyme active site, both in vivo and within an in vitro incubation is an essential requirement in rationalizing and predicting drug-drug interactions. Inhibitor accumulation within the liver, whether as a result of active transport processes or intracellular binding, may best be accounted for using hepatocytes rather than hepatic microsomes to estimate in vitro inhibitory potency. The aims of this study were to compare  $K_i$  values determined in rat liver microsomes and freshly isolated rat hepatocytes of four P450 inhibitors (clarithromycin, enoxacin, nelfinavir and saquinavir) with known hepatic transporter involvement and a range of uptake (cell-to-medium concentration ratios 20-3000) and clearance (10–1200  $\mu\text{L}/\text{min}/10^6$  cells) properties. Inhibition studies were performed using two well-established P450 probe substrates (theophylline and midazolam). Comparison of unbound  $K_i$  values showed marked differences between the two in vitro systems for inhibition of metabolism. In two cases, (clarithromycin and enoxacin – both low clearance drugs) inhibitory potency in hepatocytes markedly exceeded microsomes (10 to 20-fold) and this was consistent with their high cell-to-medium concentration ratios. For nelfinavir and saquinavir (high clearance, extensively metabolised drugs) the opposite trend was seen in the  $K_i$  values, despite very high cell-to-medium concentration ratios; stronger inhibition was evident within microsomal preparations. Hence the consequences of hepatic accumulation resulting from uptake transporters vary according to the clearance of the inhibitor. This study demonstrates that transporter-enzyme interplay can result in differences in inhibitory potency between microsomes and hepatocytes, and hence drug-drug interaction predictions, that are not always intuitive.

DMD#35824

## **Introduction**

Our understanding of the importance of hepatic transporters in controlling the disposition of drugs continues to evolve (Shitara et al., 2006; Niemi, 2007; Funk, 2008; Giacomini et al., 2010). The activity of members of the SLC and ABC families of transporter proteins may provide a mechanistic explanation for the limited success achieved for some drugs using standard (hepatic microsomal) *in vitro* experiments to predict pharmacokinetic aspects of clearance and drug-drug interaction (DDI) potential (Lam et al., 2006; Soars et al., 2007; Parker and Houston, 2008). While various theoretical scenarios involving hepatic transporters can be proposed, specific examples with experimental confirmation of an unequivocal nature has been largely restricted to the statins (Lau et al., 2006; Shitara et al., 2006; Paine et al., 2008). It appears that the consequences of hepatic transporters may not always be intuitive due to transporter-enzyme interplay and ‘transporter-like’ interactions involving other cellular processes.

The intact structural integrity of the hepatocyte may result in intracellular drug concentrations that differ from those in the surrounding medium but that are more representative of the *in vivo* situation. Assessment of the drug concentration available to the enzyme and/or transporter within the *in vitro* system is a key issue. As accumulation of drugs in hepatocytes may occur via active uptake processes and/or intracellular binding, a concentration difference may exist between hepatocyte and hepatic microsomal incubations. Whether the drug is a bound or free entity within the cell is of importance; intracellular binding to sites not involved in the metabolic process may be of little consequence, as the free concentration within the cell will be in equilibrium with the external incubation media concentration (Grime and Riley, 2006; Poirier et al., 2008;). However in the case of uptake transporters, raising the cellular concentration in excess of the incubation medium concentration will result in

DMD#35824

more drug available to the enzyme. Resolution of this situation is of importance in both the assessment of clearance and the prediction of DDIs resulting from inhibition of drug clearance.

Comparison of  $K_i$  data obtained in microsomes and hepatocytes could theoretically provide an indication of the mechanism of inhibitor accumulation. Following appropriate binding corrections, more potent hepatocyte inhibition (as evident by lower  $K_i$  values) would suggest the involvement of hepatic transporters since a higher concentration of unbound drug available for enzyme inhibition can be achieved compared to a similar incubation concentration in microsomes (Ito et al., 1998). Alternatively, similar values would indicate that any hepatic accumulation results from intracellular binding or lysosomal trapping (Grime and Riley, 2006; Hallifax and Houston, 2007). We recently demonstrated good concordance between  $K_i$  values (range 0.05-30  $\mu\text{M}$ ) determined in rat hepatic microsomes and freshly isolated hepatocytes using seven P450 inhibitors (fluconazole, fluoxetine, fluvoxamine, ketoconazole, miconazole, omeprazole and quinine) with a range of uptake properties (cell-to-medium concentration ratios 4-6000). These data suggest that the hepatic accumulation of these particular inhibitors results from intracellular binding rather than the involvement of uptake transporters, and indicate that microsomes and hepatocytes can be equivalent for determining their inhibitory potency (Brown et al., 2007). The source of these in vitro tissues was the rat to allow direct comparison of parameter values without the complication of intra-individual donor variability, which is often evident with human preparations (Hallifax et al., 2005; Rawden et al., 2005). The aims of this study were to establish general scenarios for the impact of transporters on cellular concentrations via the use of comparative inhibition in isolated hepatocytes and hepatic microsomes. Four drugs were identified for study –

## DMD#35824

CLAR, ENX, NFV, and SQV – all have known transporter involvement and show substantial hepatocellular accumulation (Sasabe et al., 1997; Yamano et al., 1999; Su et al., 2004; Maeda et al., 2007; Seithel et al., 2007; Parker and Houston, 2008; Giacomini et al., 2010). These drugs also show a range of metabolic clearance values (Table 1) allowing enzyme-transporter interplay to be assessed. The probes selected as markers of inhibition in the two systems were midazolam (for CYP3A and 2C families) and theophylline (for CYP1A family) (Kobayashi et al., 2003; Chovan et al., 2007). Comparison of inhibition parameters allows a cell:medium partition coefficient ( $K_p$ ) to be determined that can be interpreted using previously proposed models for enzyme-transporter interplay (Liu and Pang, 2005; Shitara et al., 2006). Two scenarios are evident depending upon the hepatic clearance of the inhibitor and demonstrate that microsomal:hepatocyte differences in inhibition potency and hence DDI prediction are not always intuitive.

DMD#35824

## Materials and Methods

**Chemicals.** SQV, NFV were generous gifts from Roche Products Limited (Welwyn, UK and Basel, Switzerland) 1'-hydroxymidazolam and 4-hydroxymidazolam were purchased from Ultrafine (UFC) Ltd.. All other chemicals and reagents used were of the highest grade available and were purchased from Sigma Chemicals (Poole, Dorset, UK) or BDH (Poole, Dorset, UK).

**Animal Source, Housing and Diet** Male Sprague-Dawley rats (240–260g) were obtained from the Biological Sciences Unit, Medical School, University of Manchester. They were housed in groups of two to four, in opaque boxes on a bedding of sawdust in rooms maintained at a temperature of  $20 \pm 3^\circ\text{C}$ , with a relative humidity of 40-70% and a 12 hour light/dark cycle. The animals were allowed free access CRM diet and fresh drinking water. All animal protocols were approved by University of Manchester review committee.

**Microsomal studies.** For hepatic microsomal preparations unanesthetized rats were sacrificed by cervical dislocation and washed microsomes were prepared as described previously (Hayes et al., 1995). All kinetic and inhibition studies were performed in duplicate under initial rate conditions with respect to incubation time and microsomal protein concentration. All microsomal studies were performed using three independent batches of rat liver microsomes.

*Kinetic studies.* Theophylline (50–2500  $\mu\text{M}$ ) was pre-incubated with microsomal protein at 1mg/ml and phosphate buffer (0.1M, pH 7.4) for 5 min in Eppendorf tubes in a Thermomixer (Eppendorf AG, Hamburg, Germany) set at  $37^\circ\text{C}$  and 900 rpm. Reactions were initiated by the addition of an NADPH regenerating system, and were terminated after an incubation time of 60 min by the addition of ice-cold acetonitrile containing an appropriate internal standard (S-mephenytoin). Experiments with

DMD#35824

midazolam were carried out as described previously (Brown et al., 2007) at a protein concentration of 0.2 mg/ml over 10 min (appropriately defined linear conditions).

*Inhibition studies.* Either theophylline or midazolam was incubated at concentrations equivalent to  $0.5K_M$ ,  $K_M$  and  $2K_M$ , with a range of inhibitor concentrations (at least 3 orders of magnitude to cover initial  $IC_{50}$  estimates). Incubations were performed as previously described for the microsomal kinetic studies. Fluoroquinolones have been shown to chelate divalent cations such as those present in NADPH regenerating system. For this reason, inhibition studies with ENX were performed in the presence and absence of regenerating system containing magnesium chloride, with no difference in inhibitory potency observed (data not shown).

**Hepatocyte studies.** For hepatocyte preparations unanesthetized rats were sacrificed by cervical dislocation and hepatocytes were prepared using an adaptation of the collagenase perfusion method as previously described (Hayes et al., 1995). Hepatocyte viability was determined using the trypan blue exclusion test, and only those hepatocyte preparations with viabilities greater than 85% were used. All kinetic and inhibition studies were performed in duplicate under initial rate conditions with respect to incubation time and hepatocyte density. All hepatocyte studies were performed using three independent hepatocyte preparations.

*Kinetic studies.* Theophylline (50–2500  $\mu$ M) was pre-incubated with Williams Medium E (pH 7.4) in Eppendorf tubes for 5 min in a Thermomixer (Eppendorf AG, Hamburg, Germany) set at 37°C and 900rpm. Reactions were initiated by the addition of pre-warmed hepatocytes (37°C) to give a final incubation concentration of  $1 \times 10^6$  cells/mL. Reactions were terminated after a 60 min incubation time by snap freezing in liquid nitrogen. Samples were then thawed and ice-cold acetonitrile containing an appropriate internal standard (S-mephenytoin) was added. Experiments with



DMD#35824

midazolam were carried out as described previously (Brown et al., 2007) at a cell concentration of  $0.4 \times 10^6$  cells/ml over 10 min (appropriately defined linear conditions).

***Inhibition studies.*** Either theophylline or midazolam was incubated at concentrations equivalent to  $0.5K_M$ ,  $K_M$  and  $2K_M$ , with a range of inhibitor concentrations (at least 3 orders of magnitude to cover initial  $IC_{50}$  estimates). Incubations were performed as previously described for the hepatocyte kinetic studies.

**Determination of Metabolite Concentration.** Microsomal and hepatocyte samples were vortexed and centrifuged for 10 min at 11,600 g (Eppendorf Centrifuge 5413) and an aliquot (10 $\mu$ L) of the supernatant was analysed by LC-MS/MS as previously described (Brown et al., 2007). Theophylline, 1-3 dimethyluric acid and S-mephenytoin (internal standard) were monitored using the following mass transitions: theophylline,  $m/z$  179.5>164.15 (cone voltage 95V, collision energy 20eV), 1-3 dimethyluric acid,  $m/z$  195.15>180.1 (cone voltage 90V, collision energy 20eV); S-mephenytoin,  $m/z$  217.05>188.2 (cone voltage 70V, collision energy 14eV). Methodology used for the determination of 1 and 4'-hydroxymidazolam concentrations was as previously described (Brown et al., 2007).

### **Data Analysis.**

***Kinetic data.*** All data were analysed by nonlinear regression analysis using Grafit 4 (Erithacus Software, Horley, Surrey, UK). The goodness of fit criteria used to select the model with the most appropriate fit comprised visual inspection, consideration of the randomness of residuals and the standard error of the parameters. Theophylline metabolic parameters from microsomal and hepatocyte incubations were scaled and expressed as "per g liver" using the scaling factors 60 mg protein/g liver and  $109 \times 10^6$  cells/g liver (Houston and Carlile, 1997).

DMD#35824

*Inhibition data.* IC<sub>50</sub> plots were used to distinguish between competitive and non-competitive inhibition. Using nonlinear regression, a competitive inhibition model was fitted to the data using Grafit 4 (Erithacus Software Ltd, Horley, UK) to determine the K<sub>i</sub> value of each inhibitor.

**Theoretical basis for transporter-enzyme interplay and considerations for comparing hepatocytes and hepatic microsomes.** It is problematic to estimate the unbound cellular drug concentration as only the external cellular medium can be sampled. Hence a partition coefficient (K<sub>p<sub>u</sub></sub>) for unbound drug concentration needs to be determined.

When the tissue is non-eliminating K<sub>p<sub>u</sub></sub> will reflect the true distribution or partitioning into the cell -

$$\begin{aligned} K_{p_u} &= \frac{\text{Cellular concentration}}{\text{Medium concentration}} \\ &= \frac{\text{Rate of transport in at steady state}}{\text{Rate of transport out at steady state}} \\ &= \frac{CL_{\text{uptake}} + CL_{\text{passive}}}{CL_{\text{passive}}} \end{aligned} \quad (1)$$

where CL<sub>uptake</sub> and CL<sub>passive</sub> are the cellular transport clearances by active and passive processes, respectively.

Under most experimental conditions any measurement of tissue concentration of drug represents total drug and reflects both intracellular binding and active uptake. Thus correction for intracellular binding needs to be made in order to estimate unbound cellular concentration and the impact of active uptake by transporters. One approach is to measure a cellular function that is dependent on unbound drug concentration under disrupted conditions relative to normal conditions; for example rate of transport at 4°C and 37 °C or rate of transport with and without an inhibitor.

DMD#35824

When the tissue is an eliminating tissue, like the liver, there is the additional complication of metabolism and/or biliary efflux. Hence any measure of  $Kp_u$  may reflect not only the distribution processes but also additional terms for cellular clearance (Liu and Pang, 2005; Shitara et al., 2006; Webborn et al., 2007) and is an apparent term. For the liver the term  $Kp_{u,app}$  is appropriate -

$$Kp_{u,app} = \frac{CL_{uptake} + CL_{passive}}{CL_{passive} + CL_{met}} \quad (2)$$

where  $CL_{met}$  is metabolic clearance.

To be fully descriptive the denominator of equation (2) should include a clearance term for efflux. However there is strong evidence for internalisation of the apical membrane and down regulation of these transporter proteins during the hepatocyte isolation procedure (Bow et al., 2008), hence it is not included in this model. For drugs where active uptake is important, clearance due to passive diffusion will be a minor term in equation (2). When clearance by metabolism is small then little error will be involved, however as the importance of clearance by metabolism increases (possibly exceeding the clearance for uptake)  $Kp_{u,app}$  has limited value as a distribution parameter.

An estimate of  $Kp_{u,app}$  for hepatocytes may be obtained by measuring a metabolic function. The ratio of the metabolic function in hepatocytes and microsomes would be appropriate (equation 3) given that the latter contains no cellular barrier the ratio of the rates of metabolism reflect the  $Kp_{u,app}$ .

$$Kp_{u,app} = \frac{CL_{hepatocytes}}{CL_{microsomes}} \quad (3)$$

where  $CL_{hepatocytes}$  and  $CL_{microsomes}$  refers to the metabolic clearance in the respective in vitro system.

DMD#35824

Similarly the  $K_{p_{u,app}}$  may be determined from the ratio of  $K_i$  data from microsomes and hepatocytes (equation 4).

$$K_{p_{u,app}} = \frac{K_{i,microsomes}}{K_{i,hepatocytes}} \quad (4)$$

Following appropriate binding corrections, more potent hepatocyte inhibition (or clearance) would suggest the involvement of hepatic transporters since a higher concentration of unbound drug available for enzyme inhibition can be achieved compared to a similar incubation concentration in microsomes (Ito et al., 1998). Alternatively, similar values would indicate that hepatic accumulation results from intracellular binding or lysosomal trapping.

DMD#35824

## RESULTS

**In vitro studies with theophylline and midazolam in rat freshly isolated hepatocytes in suspension and hepatic microsomes.** For theophylline, the formation of 1,3-dimethyluric acid (1,3-DMU), the major metabolite in rat (McManus et al., 1988), is best described using biphasic kinetics in both hepatocytes and microsomes (Fig.1); consistent with a high affinity, low capacity site and a low affinity, high capacity site (Table 2). When data are scaled to per g liver hepatocyte clearance is approximately 6-fold higher than microsomal clearance. The  $V_{\max}$  is double and the  $K_M$  less than half in hepatocytes when the high affinity site is compared. Also the dominance of the high affinity site is more substantial in hepatocytes than in microsomes. The high affinity  $K_M$  values were used on the basis for selection of theophylline concentrations in subsequent inhibition studies.

For midazolam, substrate concentrations of 5, 15 and 30  $\mu\text{M}$  were used in both microsomal and hepatocyte studies on the basis of previously established  $K_M$  values (Brown et al., 2007). Both midazolam metabolites (1'-OH midazolam and 4-OH midazolam) were monitored and control turnover rates are shown in Table 3. The predominant metabolite formed in both systems was found to be 4-OH midazolam - approximately 3-fold more 4-hydroxylation than 1'-hydroxylation at each midazolam concentration studied, which is consistent with previous studies (Ghosal et al., 1996; Brown et al., 2007). There is no systematic difference between the control turnover rates in the two systems once the data are expressed per g liver (Table 3). Midazolam substrate concentrations for subsequent inhibition studies were selected based on a  $K_M$  value of approximately 10  $\mu\text{M}$ .

**ENX inhibition of 1,3-DMU formation.** In liver microsomes, ENX displayed little significant inhibition of 1,3-DMU formation, even up to concentrations of 1000  $\mu\text{M}$ .

DMD#35824

However, in hepatocytes, ENX inhibition is significantly greater compared to microsomes (Table 4).  $IC_{50}$  plots for ENX in rat microsomes and hepatocytes are shown in Figs. 2A and 2B respectively, and show a progressive increase in  $IC_{50}$  value (84–256  $\mu$ M) in hepatocytes as substrate concentration is increased, consistent with a competitive inhibition mechanism. Further analysis to obtain  $K_i$  values confirmed that ENX displayed significantly more potent inhibition in hepatocytes (120  $\mu$ M) compared to microsomes (2800  $\mu$ M), corresponding to a 24-fold difference.

**CLAR inhibition of midazolam hydroxylation.** These characteristics are very similar to the inhibition of theophylline by enoxacin described above. CLAR showed weak inhibition of both pathways of midazolam metabolism in hepatic microsomes. 4-hydroxylation was more sensitive with 50% inhibition (in contrast to 30% inhibition of 1'-hydroxylation) at 1 mM CLAR. In contrast hepatocyte inhibition was substantial with both pathways showing evidence of competitive inhibition with  $IC_{50}$  values increasing from 100–650  $\mu$ M over the midazolam concentration range investigated. The  $K_i$  values for hepatocytes were 60 and 75  $\mu$ M in contrast to microsomal estimates of 650 and 1000  $\mu$ M, for 4-OH and 1'-OH, respectively. Thus the difference between in vitro systems amounted to >10-fold.

**NFV and SQV inhibition of midazolam hydroxylation.** Typical  $IC_{50}$  curves for the inhibition of the formation of 1'-OH midazolam by NFV in hepatocytes and microsomes are shown in Figs. 3A and 3B. Greater than 90% inhibition of midazolam hydroxylation was achieved at the highest concentration.  $IC_{50}$  values for both inhibition of 4-OH and 1'-OH midazolam formation were found to progressively increase in a similar fashion (0.8–8.9  $\mu$ M for hepatocytes, 0.7–2.9  $\mu$ M for microsomes) with increasing midazolam concentration indicating competitive inhibition.  $K_i$  values were calculated assuming a competitive inhibition model as 2.94

DMD#35824

and 1.16  $\mu\text{M}$  for the inhibition of 1'-OH midazolam and 4-OH midazolam formation, respectively, in hepatocytes. In microsomes substantially lower  $K_i$  values (0.46 and 0.33  $\mu\text{M}$  for the inhibition of the formation of 1'-OH midazolam and 4-OH midazolam, respectively) were found.

As with NFV, almost complete inhibition of midazolam hydroxylation by SQV was observed in both systems. SQV  $\text{IC}_{50}$  values for 1'-OH midazolam and 4-OH midazolam formation both progressively increased with increasing midazolam concentration (1.38–3.45  $\mu\text{M}$  for hepatocytes, 0.48–1.47  $\mu\text{M}$  for microsomes) again indicating competitive inhibition.  $K_i$  values calculated using a competitive inhibition model were 0.50 and 0.47  $\mu\text{M}$  for the formation of 1'-OH and 4-OH midazolam, respectively, in hepatocytes and 0.22 and 0.11  $\mu\text{M}$  for the formation of 1'-OH and 4-OH midazolam, respectively, in microsomes.

**Comparison of inhibition profiles in hepatocytes and microsomal systems.** The rank order of  $K_i$  values in rat hepatocytes and microsomes is essentially similar for the four inhibitors (Table 4). However marked differences in the ratio of  $K_i$  values between the systems are seen, ranging from 0.2 for NFV to 23 for ENX. Values of  $f_u$  for each inhibitor in microsomes were determined experimentally (see Table 1). These values were used to calculate the intracellular fraction unbound for the hepatocyte studies (Kilford et al., 2008). Both sets of values are listed in Table 1. Under the incubation conditions used the ratios of the unbound fractions in the microsomal and hepatocyte incubations were within the range 0.98-1.2; therefore no corrections were made for the relative nonspecific binding in the two in vitro systems for any of the four inhibitors.

For each inhibitor the ratio of the microsomal to hepatocellular  $K_i$  value was used as an estimate of  $K_{p,u,app}$ . Table 5 compares these values with other independently

DMD#35824

determined  $K_p$ s, expressed both in terms of total and unbound drug concentrations (the latter obtained from permeability studies). With the exception of ENX, no concordance was evident, rather an approximate negative correlation between  $K_{p_{u,app}}$  and  $K_p$  based on total drug concentration. From the  $K_{p_{u,app}}$  two groupings are evident depending on whether  $K_{p_{u,app}}$  values are above or below unity. Both groups are also distinct in metabolic clearance – first being low clearance (<3 mL/min/g liver) whereas the second are high clearance drugs (>50 mL/min/g liver).

**Interplay of metabolism and transporters on  $K_{p_u}$ .** The relationship describing  $K_{p_{u,app}}$  in terms of uptake, passive permeability and metabolism (equation 2), has been derived by others (Liu and Pang, 2005; Shitara et al., 2006) and was used to generate a 3-dimensional surface for  $K_{p_{u,app}}$  to illustrate the interplay of these clearance terms. Fig. 4 shows the result for a range of uptake and metabolic clearances (0.001–10 mL/min/ $10^6$  cells) for drugs with intermediate (0.1 mL/min/ $10^6$  cells) passive permeability.

Taking as a starting point the case where clearances by uptake and metabolism are low and equal (0.0001 mL/min/ $10^6$  cells) and less than passive permeability, a  $K_{p_{u,app}}$  of unity results. For compounds with a slow rate of metabolism, an increase in uptake clearance results in the expected progressive increase in  $K_{p_{u,app}}$  from one to several thousand. Considering the same range of uptake clearance for compounds with faster metabolic clearances, then  $K_{p_{u,app}}$  values are lower but show a similar increase. At the extreme case of uptake clearance of 10 mL/min/ $10^6$  cells, the progressive decrease in  $K_{p_{u,app}}$  as clearance via metabolism increases from a low value to unity. It is evident from this surface that only certain combinations of clearances for uptake and metabolism results in  $K_{p_{u,app}}$  greater than one. As these two processes are



## DMD#35824

counteracting there are a number of situations where  $K_{p_{u,app}}$  less than one result although there is significant active uptake.

The slope of the surface is dependent upon the permeability value assigned for the passive process; an intermediate permeability (0.1 mL/min/ $10^6$  cells) is shown in Fig. 4, the use of a low permeability (0.001 mL/min/ $10^6$  cells) results in a steeper surface, and for a high permeability (10 mL/min/ $10^6$  cells) the surface is almost flat.

It is useful to consider the surface (Fig. 4) in terms of two halves separated by the diagonal at  $K_{p_{u,app}}$  of unity for particular combinations of parameters. Above the diagonal  $K_{p_{u,app}}$  is greater than one and compounds with clearance values within this half will be characterised by hepatic uptake that is metabolism rate limited (e.g. ENX and CLAR). Compounds with properties corresponding to a position below the diagonal are those with transport rate limited uptake (e.g. NFV and SQV). With the second scenario, for low permeability compounds with high metabolic clearance, there is no build up of drug concentration within the cell, therefore although transporters would be expected to result in high  $K_{p_u}$ ; the rate limiting step for drug disposition in the in vitro system is cellular uptake. However when the latter process is substantially less than metabolic clearance, there is no cellular accumulation and  $K_{p_{u,app}}$  provides no guide to the importance of the transporter uptake. This contrasts with the first scenario for low permeability compounds where the impact of transporters is fully evident and  $K_{p_{u,app}}$  reflects  $K_{p_u}$ .

DMD#35824

## DISCUSSION

For all four compounds, inhibition was clearly evident in the hepatocyte preparations and this is consistent with in vivo studies in both humans and rats (Edwards et al., 1988; Olkkola et al., 1993; Davis et al., 1994; Yamaji et al., 1999; Yamano et al., 1999; Shibata et al., 2000). The two protease inhibitors studied, SQV and NFV were very potent inhibitors of midazolam hydroxylation with  $K_i$  values equal or less than 1  $\mu\text{M}$ . In the case of ENX and CLAR inhibition  $K_i$  values were much less potent in the region of 100  $\mu\text{M}$ . All compounds are known to be substrates for the SLC transporter proteins (Sasabe et al., 1997; Yamano et al., 1999; Su et al., 2004; Maeda et al., 2007; Seithel et al., 2007; Giacomini et al., 2010), thus there was an expectation that hepatocytes would show higher sensitivity to inhibition than microsomes. Whilst this scenario was evident for ENX and CLAR, the opposite tendency was seen for the two protease inhibitors.

The marker substrates used in this study were theophylline and midazolam. They were selected as classic substrates for human P450s, namely CYP1A2 and CYP3A4. In the case of midazolam this CYP preference is essentially maintained in the rat particularly for the 4-hydroxylation pathway, however in the case of the 1'-hydroxylation pathway there is also a contribution from CYP2C11 and 2C13 (Chovan et al., 2007). Theophylline appears to be a more promiscuous substrate in terms of rat cytochrome P450s (McManus et al., 1988) however a high correlation has been reported between the in vivo clearance of theophylline and in vitro ethoxyresorufin O-deethylation (a classic CYP1A substrate reaction, Matthews and Houston, 1990).

It has been suggested by Kobayashi et al., (2005) that there may be possible involvement of organic anion transporter inhibition in the interaction between theophylline and erythromycin. This suggestion was based on studies in *Xenopus*

DMD#35824

ocytes demonstrating that both compounds have similar  $K_M$  values and show competitive inhibition. Our data on theophylline metabolism in hepatocytes and microsomes do not confirm this proposal. Although clearance is higher in the cellular system this is associated with substantial increases in  $V_{max}$ , a kinetic parameter not sensitive to substrate concentration changes. However we cannot discount completely the possibility of a transporter component contributing to the theophylline-enoxacin interaction.

ENX and CLAR inhibition in microsomes was very weak and only observable at very high concentrations. Our estimates of  $K_i$ , while somewhat imprecise, are certainly greater than 1000  $\mu\text{M}$ . In contrast using hepatocytes the inhibition properties of both compounds were easily characterized; classic  $\text{IC}_{50}$  profiles were obtained and  $\text{IC}_{50}$  values showed a progressive increase with substrate concentration indicating competitive inhibition. The  $K_i$  value in hepatocytes for ENX and CLAR were approximately 100  $\mu\text{M}$ , i.e. at least 10 times lower than seen in microsomes.

The inhibitory properties of both ENX and CLAR in microsomes and hepatocytes contrast markedly with that observed for the protease inhibitors. In microsomes, SQV and NFV were shown to be potent inhibitors of the CYP3A-mediated metabolism of midazolam. The relative inhibitory potency was very similar for both 1'-OH midazolam and 4-OH midazolam formation; the formation of 4-OH midazolam was found to be more sensitive to inhibition than 1'-OH midazolam. SQV and NFV exhibited competitive inhibition and no evidence of partial inhibition. The inhibitory potency for the inhibition of 1'-OH midazolam observed in rat microsomes is comparable to results published by Shibata et al., (2002).

The inhibition potency of NFV and SQV observed in rat hepatocytes was less than that evident with microsomes for both metabolites;  $K_i$  values ranged from 0.47 to 2.94

DMD#35824

$\mu\text{M}$  and 0.11 to 0.46  $\mu\text{M}$  for the hydroxylation of midazolam in hepatocytes and microsomes, respectively. This was particularly apparent in the case of NFV and the trend is reflected in SQV  $K_i$  values.

Both ENX and CLAR show low clearance by the liver and in the case of ENX renal clearance is equally important in the overall elimination of this compound in vivo in both rats and man (Paton and Reeves, 1988; Davis et al., 1994). In contrast the hepatic clearance of the protease inhibitors is very high (Shibata et al., 2000; Parker and Houston, 2008). We have studied this in some detail in vitro and have demonstrated that in hepatocytes metabolic clearance is transporter rate limited (Parker and Houston, 2008). Thus there is a clear distinction between these two classes of compound in terms of their hepatic metabolic clearance characteristics. This behaviour is consistent with the differences reported here in terms of  $K_i$  values and the resulting  $K_{p,u,app}$ . Interestingly the ratio of microsomal to hepatocyte  $K_M$  values (Parker and Houston, 2008) is similar to the corresponding ratio of  $K_i$  values (Table 5).

The data reported herewith contrasts with our previous publication (Brown et al., 2007) where we were able to show that the hepatic accumulation of seven P450 inhibitors (fluconazole, fluoxetine, fluvoxamine, ketoconazole, miconazole, omeprazole and quinine) resulted from intracellular binding rather than any involvement of transporters. For these compounds we demonstrated good concordance between  $K_i$  values (range 0.05 to 30  $\mu\text{M}$ ) in microsomes and hepatocytes despite the differing importance of hepatic accumulation observed for these compounds ( $K_p$  values ranging from 4 to 6000). In contrast Grime et al., (2008) demonstrated a 5-fold difference in inhibition between recombinant rat P450s and isolated rat hepatocytes for four lipophilic carboxylic acids including atorvastatin and

DMD#35824

pitavastatin. As with the present study there was a disconnect between the change in the  $K_i$  value between these systems and the extent of hepatic accumulation (approximately 1000-fold). Thus the authors concluded that there was high intracellular binding resulting in accumulation and proposed  $K_{p_u}$  values would be in the order of 5, a similar situation to that observed with NFV and SQV (Parker and Houston, 2008).

The  $IC_{50}$  curves reported by Grime et al., (2008) were somewhat flat, contrasting with the traditional sigmoidal shape, and the reasons for this are open to question. These authors discussed the scenario where the affinity constant for the transporter may be of a similar value to the  $K_i$  and showed by simulation that this can result in a relatively flat  $IC_{50}$  profile. However a similar behaviour was reported in analogous experiments with recombinant systems. Comparison of inhibition properties in individual recombinant P450s with hepatocytes, where the full complement of P450 enzymes are present and hence may contribute to the observed inhibition effect, is problematic.

In conclusion, our observations indicate that the use of  $K_i$  values (or indeed  $K_M$ ) in hepatocytes and microsomes as an indication of active transport may not be straightforward. For ENX and CLAR, the observations reported here are as expected based on information available on the active transport of these compounds into hepatocytes. In contrast the observations with the protease inhibitors were not intuitive, however consideration of hepatic clearance allows these observations to be rationalized. Use of a simple model to describe the hepatocellular processes of metabolism, uptake and passive permeability illustrates the interplay which defines  $K_{p_u,app}$ . Also it provides a rational for two inhibition scenarios resulting from whether the inhibitor displays metabolic or uptake rate limited clearance and highlights the

DMD#35824

potential shortcomings of using subcellular fractions such as microsomes rather than hepatocytes to predict likely DDI in vivo.

DMD#35824

### **Acknowledgements**

The authors would like to thank Sue Murby and Dr Raj Badhan for valuable assistance with the LC-MS/MS and simulation work.

DMD#35824

## References

Brown HS, Chadwick A, and Houston JB (2007) Use of Isolated Hepatocyte Preparations for Cytochrome P450 Inhibition Studies: Comparison with Microsomes for  $K_i$  Determination. *Drug Metab Dispos* **35**:2119–2126.

Bow DAJ, Perry JL, Miller DS, Pritchard JB and Brouwer KLR (2008) Localization of P-gp (Abcb1) and Mrp2 (Abcc2) in freshly isolated rat hepatocytes. *Drug Metab Dispos* **36**:198-202.

Chovan JP, Ring SC, Yu E, and Baldino JP (2007) Cytochrome P450 probe substrate metabolism kinetics in Sprague Dawley rats. *Xenobiotica* **37**:459–473.

Davis JD, Aarons L and Houston JB (1994) Relationship between enoxacin and ciprofloxacin plasma concentrations and theophylline disposition. *Pharm Res* **11**: 1424-1428.

Edwards DJ, Bowles SK, Svensson CK and Rybak MJ (1988) Inhibition of drug metabolism by quinolone antibiotics. *Clin Pharmacokin* **15**: 194-204.

Funk C (2008) The role hepatic transporters in drug elimination. *Expert Opin Drug Metab Toxicol* **4**: 363-379.

Ghosal A, Satoh H, Thomas PE, Bush E and Moore D (1996) Inhibition and kinetics of cytochrome P450 3A activity in microsomes from rat, human, and cDNA-expressed human cytochrome, P450. *Drug Metab Dispos* **24**: 940-947.



DMD#35824

Giacomini, KM, Huang SM, Tweedie DJ, Benet LZ, Brouwer KLR, Chu X, Dahlin A, Evers R, Fischer V, Hillgren KM, Hoffmaster KA, Ishikawa T, Keppler D, Kim RB, Lee CA, Niemi M, Polli JW, Sugiyama Y, Swaan PW, Ware JA, Wright SH, Yee SW, Zamek-Gliszczynski MJ, Zhang L (2010) Membrane transporters in drug development. *Nature Rev Drug Discovery* **9**:215-236.

Grime K and Riley RJ (2006) The impact of in vitro binding on in vitro-in vivo extrapolations, projections of metabolic clearance and clinical drug-drug interactions. *Curr Drug Metab* **1**:251-264.

Grime K, Webborn PJH and Riley RJ (2008) Functional consequences of active hepatic uptake on cytochrome P450 inhibition in rat and human hepatocytes. *Drug Metab Dispos* **36**: 1670-1678.

Hallifax D, Rawden HC, Hakooz N and Houston JB (2005) Prediction of metabolic clearance using cryopreserved human hepatocytes: kinetic characteristics for five benzodiazepines. *Drug Metab Dispos* **33**: 1852-1858.

Hallifax D and Houston JB (2007) Saturable uptake of lipophilic amine drugs into isolated hepatocytes: Mechanisms and consequences for quantitative clearance prediction. *Drug Metab Dispos* **35**: 1325-1332.

DMD#35824

Hayes KA, Brennan B, Chenery R and Houston JB (1995) In vivo disposition of caffeine predicted from hepatic microsomal and hepatocyte data. *Drug Metab Dispos* **23**: 349-53.

Houston JB and Carlile DJ (1997) Prediction of hepatic clearance from microsomes, hepatocytes, and liver slices. *Drug Metab Rev* **29**:891-922.

Ito K, Iwatsubo T, Kanamitsu S, Nakajima Y, and Sugiyama Y (1998) Quantitative prediction of *in vivo* drug clearance and drug interactions from *in vitro* data on metabolism, together with binding and transport. *Annu Rev Pharmacol Toxicol* **38**:461-499.

Kilford PJ, Gertz M, Houston JB and Galetin A (2008) Hepatocellular binding of drugs: correction for unbound fraction in hepatocyte incubations using microsomal binding or drug lipophilicity data. *Drug Metab Dispos* **36**: 1194-1197.

Kobayashi K, Urashima K, Shimada N and Chiba K (2003) Selectivities of human cytochrome P450 inhibitors towards rat P450 isoforms: study with cDNA-expressed systems of the rat. *Drug Metab Dispos* **31**: 833-836.

Kobayashi K, Sakai R, Ohshiro N, Ohbayashi M, Kohyama N and Yamamoto T (2005) Possible involvement of organic anion transporter 2 on the interaction of theophylline with erythromycin in the human liver. *Drug Metab Dispos* **33**: 619-622.

DMD#35824

Lam JL, Okochi H, Huang Y and Benet LZ (2006) In vitro and in vivo correlation of hepatic transporter effects on erythromycin metabolism: characterising the importance of transporter-enzyme interplay. *Drug Metab Dispos* **34**: 1336-1344.

Lau YY, Okochi H, Huang Y and Benet LZ (2006) Multiple transporters affect the disposition of atorvastatin and its two active hydroxyl metabolites: application of *in vitro* and *ex situ* systems. *J Pharmacol Exp Ther* **316**: 762-771.

Liu L and Pang KS (2005) The roles of transporters and enzymes in hepatic drug processing. *Drug Metab Dispos* **33**:1-9.

Maeda T, Takahashi K, Ohtsu N, Oguma T, Ohnishi T, Atsumi R and Tamai I (2007) Identification of influx transporter for the quinolone antibacterial agent levofloxacin. *Mol Pharmacol* **4**: 85-95.

Matthew DE and Houston, JB (1990) Drug metabolising capacity in vitro and in vivo. 1. Correlations between hepatic microsomal mono-oxygenase markers in  $\beta$ -naphthoflavone-induced rats *Biochem Pharmacol* **40**:743-749.

McManus ME, Miners JO, Gregor D, Stupans I and Birkett DJ (1988) Theophylline metabolism by human, rabbit and rat liver microsomes and by purified forms of cytochrome P450. *J Pharm Pharmacol* **40**: 388-391.

Niemi M (2007) Role of OATP transporters in the disposition of drugs. *Pharmacogenomics* **8**:787-802.

DMD#35824

Olkkola KT, Aranko K, Luurila H, Hiller A, Saarnivaara L, Himberg JJ and Neuvonen PJ (1993) A potentially hazardous interaction between erythromycin and midazolam. *Clin Pharmacol Ther* **53**: 298-305.

Paine SW, Parker AJ, Gardiner P, Webborn PJH, and Riley RJ (2008) Prediction of the pharmacokinetics of atorvastatin, cerivastatin, and indomethacin using kinetic models applied to isolated rat hepatocytes. *Drug Metab Dispos* **36**:1365–1374.

Parker AJ and Houston JB (2008) Rate-Limiting Steps in Hepatic Drug Clearance: Comparison of Hepatocellular Uptake and Metabolism with Microsomal Metabolism of Saquinavir, Nelfinavir, and Ritonavir. *Drug Metab Dispos* **36**:1375–1384.

Paton JH and Reeves DS (1988) Fluoroquinolone antibiotics-microbiology, pharmacokinetics and clinical use. *Drugs* **36**:193-228.

Poirier A, Lave T, Portmann R, Brun ME, Senner F, Kansy M, Grimm HP and Funk C (2008) Design, data analysis and simulation of in vitro drug transport kinetic experiments using a mechanistic in vitro model. *Drug Metab Dispos* **36**: 2434-2444.

Rawden HC, Carlile DJ, Tindall A, Hallifax D, Galetin A, Ito K and Houston JB (2005) Microsomal prediction of in vivo clearance and associated inter individual variability of six benzodiazepines in humans. *Xenobiotica* **35**: 603-625.

DMD#35824

Sasabe H, Terasaki T, Tsuji A and Sugiyama Y (1997) Carrier-mediated hepatic uptake of quinolone antibiotics in the rat. *J Pharm Exp Ther* **282**:162-171.

Seithel A, Eberl S, Singer K, Auge D, Heinkele G, Wolf NB, Dorje F, Fromm MF and Konig J (2007) The influence of macrolide antibiotics on the uptake of organic anions and drugs mediated by OATP1B1 and OATP1B3. *Drug Metab Dispos* **35**: 779-786.

Shibata N, Matsumura Y, Okamoto H, Kawaguchi Y, Ohtani A, Yoshikawa Y and Takada K (2000) Pharmacokinetic interactions between HIV-1 protease inhibitors in rats: study on combinations of two kinds of HIV-1 protease inhibitors. *J Pharm Pharmacol* **52**:1239-1246.

Shitara Y, Horie T and Sugiyama Y (2006) Transporters as a determinant of drug clearance and tissue distribution. *Eur J Pharm Sci* **27**:425-446.

Soars MG, McGinnity DF, Grime K and Riley RJ (2007) The pivotal role of hepatocytes in drug discovery. *Chemico-Biological Interactions* **168**: 2–15.

Su Y, Zhang X and Sinko PJ (2004) Human organic anion-transporting polypeptide OATP-A (SLC21A3) acts in concert with P-glycoprotein and multidrug resistance protein 2 in the vectorial transport of saquinavir in Hep G2 cells. *Mol Pharm* **1**:49-56.

DMD#35824

Webborn PJH, Parker AJ, Denton RL and Riley RJ (2007) In vitro-in vivo extrapolation of hepatic clearance involving active uptake: theoretical and experimental aspects. *Xenobiotica* **37**: 1090-1109.

Yamaji H, Matsumura Y, Yoshikawa Y and Takada K (1999) Pharmacokinetic interactions between HIV-protease inhibitors in rats. *Biopharm Drug Dispos* **20**:241-247.

Yamano K, Yamamoto K, Kotaki H, Takedomi S, Matsuo H, Sawad Y and Iga T (1999) Correlation between in vivo and in vitro hepatic uptake of metabolic inhibitors of cytochrome P450 in rats. *Drug Metab Dispos* **27**: 1225-1231.

DMD#35824

### **Footnotes**

This work was partially funded by a consortium of pharmaceutical companies (GlaxoSmithKline, Lilly, Novartis, Pfizer and Servier) within the Centre for Applied Pharmacokinetic Research at the University of Manchester. AJW was financially supported by BBSRC CASE studentship with Roche Products Ltd.

Current addresses: <sup>1</sup>CVGI Discovery Drug Metabolism and Pharmacokinetics, AstraZeneca, Alderley Park, Macclesfield, Cheshire, UK; <sup>2</sup>Department of Discovery DMPK, AstraZeneca R&D Charnwood, Loughborough, UK; <sup>3</sup>School of Pharmacy and Biomedical Sciences, University of Central Lancashire, Preston, UK.

DMD#35824

## Figure Legends

Fig 1. 1,3-dimethyluric acid (1,3-DMU) formation from theophylline over a range of substrate concentrations in rat hepatocytes (•) and hepatic microsomes (o) Rates are expressed by g liver to allow direct comparison of the two systems. Typical sets of data are shown together with the lines of best fit using a two-site Michaelis-Menten equation.

Fig. 2 Relationship between inhibition of 1,3-dimethyluric acid (1,3-DMU) formation from theophylline (expressed as % of control activity) and inhibitor concentration for enoxacin in freshly isolated rat hepatocytes in suspension (A) and rat liver microsomes (B). Typical  $IC_{50}$  plots are shown for theophylline concentrations equivalent to  $0.5K_M$  (•),  $K_M$  (▲) and  $2K_M$  (□) and the lines shown are the lines of best fit using the standard  $IC_{50}$  equation.

Fig. 3 Relationship between inhibition of 1'-hydroxylation of midazolam (expressed as % of control activity) and inhibitor concentration for nelfinavir in suspended rat hepatocytes (A) and rat liver microsomes (B), Typical  $IC_{50}$  plots are shown for midazolam concentrations of 5 (•), 15 (▲) and 30 (□)  $\mu M$  and the lines shown are the lines of best fit using the standard  $IC_{50}$  equation.

Fig. 4 Surface plot to illustrate the interplay between uptake and metabolic clearances in defining  $K_{p_{u,app}}$  for intermediate permeability drugs ( $0.1 \text{ mL/min}/10^6 \text{ cells}$ ). Simulations based on equation 2 for a range of uptake and metabolic clearances.



DMD#35824

**Table 1: Binding and clearance properties of four inhibitors selected for study**

<b>Inhibitor</b>	<b>K<sub>p</sub></b>	<b>CL<sub>ints, heps</sub> (<math>\mu\text{L}/\text{min}/10^6</math> cells)</b>	<b>fu,mic (at 1mg/ml)</b>	<b>fu,heps (at <math>10^6</math> cells)<sup>d</sup></b>
Enoxacin	20 <sup>a</sup>	9.6 <sup>c</sup>	0.99 <sup>c</sup>	0.99
Clarithromycin	22 <sup>a</sup>	16.9 <sup>c</sup>	0.81 <sup>c</sup>	0.86
Saquinavir	306 <sup>b</sup>	486 <sup>b</sup>	0.093 <sup>b</sup>	0.14
Nelfinavir	3352 <sup>b</sup>	1290 <sup>b</sup>	0.022 <sup>b</sup>	0.035

<sup>a</sup>Yamano et al., 1999

<sup>b</sup>Parker and Houston, 2008

<sup>c</sup>Alder, J, and Davis, JD, unpublished data

<sup>d</sup>calculated from Kilford et al., 2008

DMD#35824

**Table 2: Formation kinetics of 1,3-Dimethyluric acid from theophylline in rat hepatocytes and hepatic microsomes**

<b>In vitro system</b>	<b>K<sub>M,1</sub> (mM)</b>	<b>K<sub>M,2</sub> (mM)</b>	<b>V<sub>max1</sub> (nmol/min/ g liver)</b>	<b>V<sub>max2</sub> (nmol/min/ g liver)</b>	<b>CL<sub>int1</sub> (μL/min/ g liver)</b>	<b>CL<sub>int2</sub> (μL/min/g liver)</b>
Microsomes	0.29 ± 0.08	10.3 ± 4.2	1.5 ± 0.4	13.9 ± 4.0	5.4 ± 2.8	1.4 ± 0.3
Hepatocytes	0.11 ± 0.04	5.4 ± 3.6	3.9 ± 1.6	8.0 ± 2.8	35.0 ± 8.7	2.2 ± 1.6

DMD#35824

**Table 3: Turnover rates for midazolam in suspended rat hepatocytes and hepatic microsomes**

Midazolam concentration ( $\mu\text{M}$ )	Hepatocellular rate of formation (pmol/min/g liver)			Microsomal rate of formation (pmol/min/g liver)		
	1'-OH midazolam	4-OH midazolam	Ratio 4-OH/1'-OH	1'-OH midazolam	4-OH midazolam	Ratio 4-OH/1'-OH
5	$5.3 \pm 1.3$	$12.7 \pm 4.2$	2.4	$7.6 \pm 2.8$	$19.9 \pm 7.6$	2.6
15	$9.9 \pm 1.5$	$25.4 \pm 6.9$	2.6	$9.0 \pm 4.1$	$33.9 \pm 12.8$	2.9
30	$11.2 \pm 1.4$	$29.6 \pm 7.9$	2.6	$12.5 \pm 4.3$	$37.2 \pm 12.9$	2.9

DMD#35824

**Table 4:  $K_i$  values for inhibition of 1,3-dimethyluric acid formation from theophylline and inhibition of 1'- and 4-hydroxylation of midazolam in rat hepatocytes and hepatic microsomes**

<b>Inhibitor</b>	<b>Substrate</b>	<b>Pathway</b>	<b>Hepatocyte <math>K_i</math> (<math>\mu\text{M}</math>)</b>	<b>Microsomal <math>K_i</math> (<math>\mu\text{M}</math>)<sup>a</sup></b>
Enoxacin	Theophylline	1,3-dimethyluric acid	120 $\pm$ 65	2800 $\pm$ 1200
Clarithromycin	Midazolam	1'-hydroxylation	75 $\pm$ 24	1000 $\pm$ 100
		4-hydroxylation	60 $\pm$ 30	650 $\pm$ 80
Saquinavir	Midazolam	1'-hydroxylation	0.50 $\pm$ 0.035	0.22 $\pm$ 0.07
		4-hydroxylation	0.47 $\pm$ 0.099	0.11 $\pm$ 0.01
Nelfinavir	Midazolam	1'-hydroxylation	2.94 $\pm$ 1.02	0.46 $\pm$ 0.1
		4-hydroxylation	1.16 $\pm$ 0.49	0.33 $\pm$ 0.02

Mean data of 3 preparations  $\pm$  SD, each preparation studied with 3 substrate concentrations over a range of inhibitor concentrations

<sup>a</sup> Statistical difference between hepatocytes and microsomes ( $p < 0.01$ )

DMD#35824

**Table 5: Comparison of hepatocyte and microsomal parameters for distribution, inhibition and metabolism**

Inhibitor	K <sub>p</sub>	K <sub>p<sub>u</sub></sub>	K <sub>i</sub> - microsomal to hepatocellular ratio		
			1'-OH midazolam	4-OH midazolam	Theophylline hydroxylation
Enoxacin	20 <sup>a</sup>	-	-	-	23
Clarithromycin	22 <sup>a</sup>	6.1 <sup>c</sup>	13	11	-
Saquinavir	306 <sup>b</sup>	6.8 <sup>b</sup>	0.44	0.23	-
Nelfinavir	3352 <sup>b</sup>	5.7 <sup>b</sup>	0.16	0.28	-

<sup>a</sup>Yamano et al., 1999

<sup>b</sup>Parker and Houston, 2008

<sup>c</sup>Yabe, Y, unpublished data

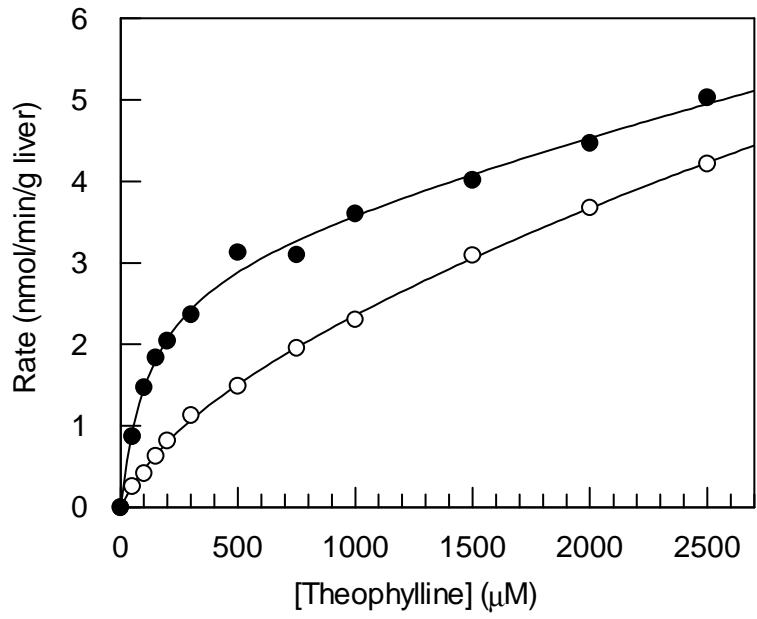


Fig. 1

Fig. 2

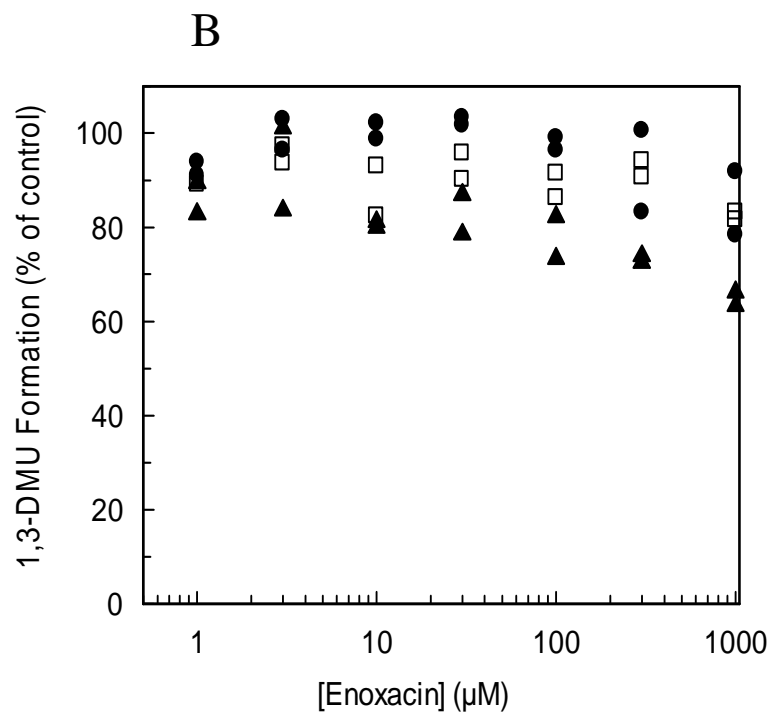
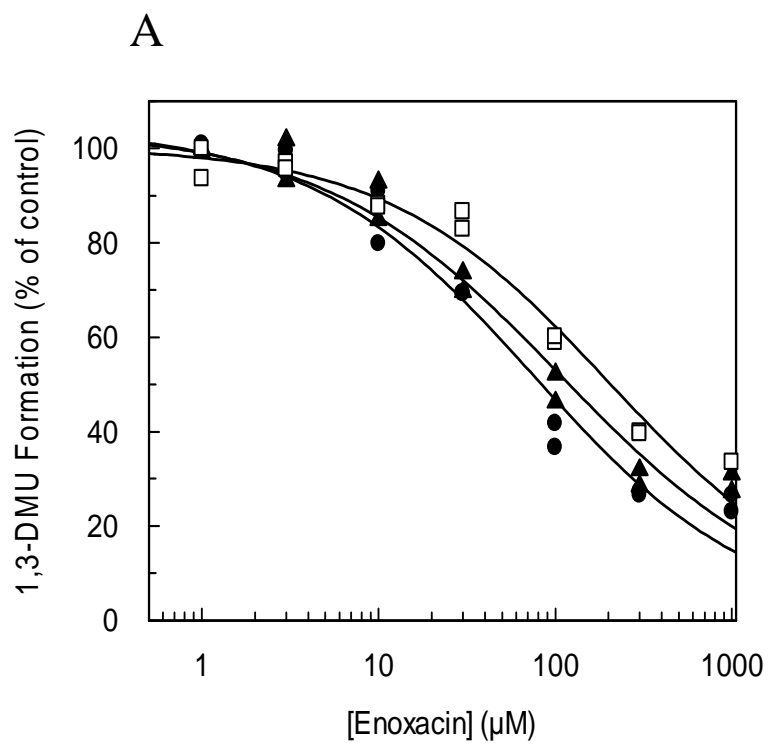


Fig. 3

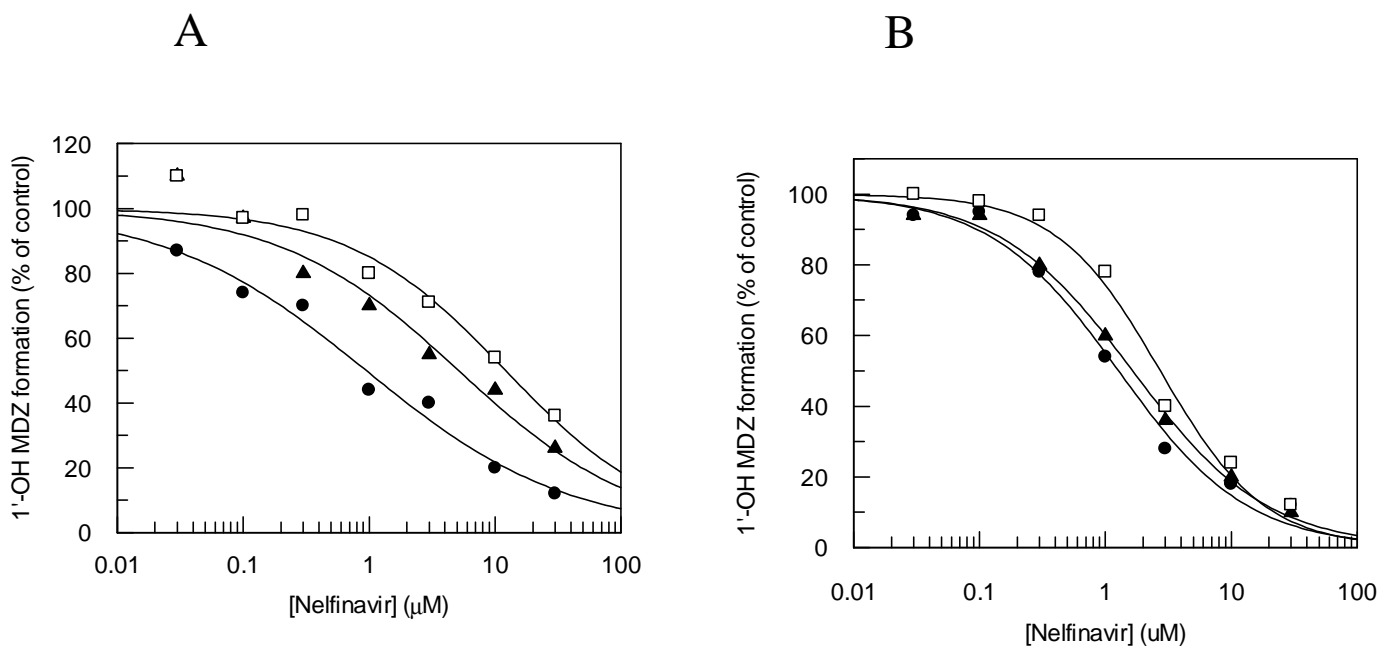




Fig. 4

